Sensors & Transducers, Vol. 261, Issue 2, June 2023, pp. 15-24

www.sensorsportal.com

Sensors & Transducers

Published by IFSA Publishing, S. L., 2023
http://www.sensorsportal.com

Multi-Complex Robot Interaction with Homothetic Human Feedback in a Virtual Environment

[1, *] Taha HOUDA, [2] Ayman BEGHDADI, [2] Lotfi BEJI and [2] Ali AMOURI

[1] ESIEE-IT, 8 Rue Pierre de Coubertin, 95300 Pontoise, France
[2] IBISC EA 4526 Laboratory, University of Paris-Saclay, 91080 Evry-Courcouronnes, France
[1] Tel.: +33788596730
E-mail: thouda@esiee-it.fr, aymanaymar.beghdadi@univ-evry.fr,
lotfi.beji@univ-evry.fr, ali.amouri@univ-evry.fr

Received: 10 April 2023 Accepted: 7 June 2013 Published: 26 June 2023

Abstract: In recent years, the interaction between mechatronic systems and humans, such as human-robot and robot-robot interaction, has gained considerable momentum. The integration and coupling of virtual reality and virtual reality has become very important in Industry 4.0 and 5.0 in general. Motion simulators present a concrete system for the integration and interaction of mechatronic subsystems. Different types of simulators are increasingly being integrated in the various application areas in aviation, at sea and on land. The extension of the application of the simulator in the field of the sport and in particular of the functional rehabilitation has taken a great interest in the public and private sectors. In this context, our team objective is to study the design and to realize a simulator mastering all the low level elements in order to explore the integration of a virtual environment in a complex interactive robotic system. In this paper, we aim to study robot-robot interaction and validate the accuracy and shape tracking of motion perception in skiing for simulator users using the Nao robot.

Keywords: Handiski, Motion simulator, Robot-Robot interaction, Motion cueing algorithm, Humanoid robot, Disabled people, Washout filter.

1. Introduction

Handiski (Handicap, Alpine Skiing), means the adaptation of alpine skiing practice to people with disabilities, is a new sport that arouses a huge interest among enthusiasts, who enjoy practicing it every year. However, there are many restrictions to ski training, especially for people with disabilities. There are environmental dependencies, as skiing requires a good amount of snow and slopes, which limits the sport to certain seasons and suitable resorts.

For that, the ski simulators are becoming increasingly popular in the sliding sports industry due to their ability to replicate real-world sliding conditions and provide users with an immersive experience. They use advanced technologies to replicate the sliding motions, gravity, and vibrations of snow, such as the Motion Cueing Algorithm (MCA) [1]. These simulators can be used for sports training, injury recovery, mental preparation, and functional rehabilitation [2]. Ski simulators can also be coupled with virtual reality to increase immersion and human sensation [3]. To the best of our knowledge, all existing ski simulators use only a 2 DoF mechatronic system which is not sufficient to reproduce all the movements of the skier. We propose a VR-based indoor ski high degree of freedom training system 8 DoF simulator. Using this training system, we replay the movement of an expert skier recorded on a virtual track and we can reproduce this movement in the simulator as faithfully as possible.

MCAs are computer-based techniques used to simulate the effects of motion in skiers. These algorithms are designed to mimic the physical sensation of motion, such as acceleration and deceleration, by adjusting the visual cues that the skier receives. These cues can include changes in the skier's body position, speed, and slope angle, as well as changes in the skier's body position and motion itself. The MCA produces a trajectory that maximizes human sensation while respecting the physical limitations of the simulator.

In general, motion simulators are a multidisciplinary engineering system that can be traced back to the early 20th century. One of the first such devices was the Gough-Stewart platform [4], which was primarily used for military training and research [5, 6]. This platform has a six-degree-of-freedom range of motion. The upper platform can be mounted in a cockpit and uses a combination of rotating and linear actuators to simulate motion. Over time, motion simulators have evolved significantly thanks to advances in technology and engineering. The hybrid platform was introduced by coupling the Gough-Stewart platform with the X-rail or XY table to create a more realistic and immersive experience. For example, the Renault Driving Simulator, which adds an X-rail at Technocentre Renault, France [7] and the National Advanced Driving Simulator (NADS) at IOWA, USA [8] and the XY-6 DOF from IBISC Laboratory [9], which adds an XY table. The aim of the project is to contribute to technological progress in the field of rehabilitation and to provide a unique approach to physiotherapy for people with disabilities. For that, a low-cost simulator called the XY-6 DoF was designed and built from scratch in the IBISC laboratory [10]. The XY-6 DoF simulator is characterized by being completely open and allowing low-level access to the platform, which enables the development and adaptation of new algorithms.

In this paper, we aim to validate the precision and shape tracking of motion perception in skiing for simulator users and evaluate the effectiveness of the simulator as a rehabilitation tool. The humanoid robot Nao has a skeletal structure that mimics a human, which enables it to emulate human-like motion patterns. It is also equipped with appropriate sensors to perceive and interact with its environment. The Nao humanoid robot has been used to interact with humans for many years and has proven its efficiency. Nowadays, it is more and more used in robot-robot interaction, replacing humans, such as in the paper [11], which uses the Nao robot for gesture-based interaction between humans and multi-robot swarms. For all these reasons and for human safety, Nao is a good choice to replace humans with a good similarity.

This paper is organized as follows: Section 2 describes the technical and system architecture of the XY-6 DoF simulator. Section 3 discusses the robot coupling and interaction between the XY-6 DoF and the humanoid robot Nao. Finally, Section 4 presents simulations and discussions.

2. Technological Presentation

The ski simulator system integrates complex multi-robot interaction through the XY-6 DoF platform and the Nao humanoid robot. The XY-6DoF simulator presented in Fig. 1 and Fig. 2, was designed and developed from scratch by our research team in the IBISC laboratory [11].

The association of these two complex robotic systems with very different characteristics required a deep understanding of the low and high-level software and hardware system. The XY-6DoF simulator presented in Fig.1 and Fig.2, was designed and developed from scratch by our research team in the IBISC laboratory [11].

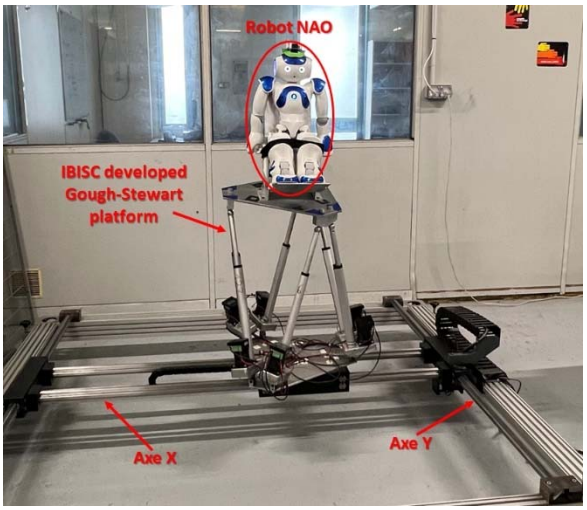


Fig. 1. The XY-6 DoF physical ski simulator with NAO robot.

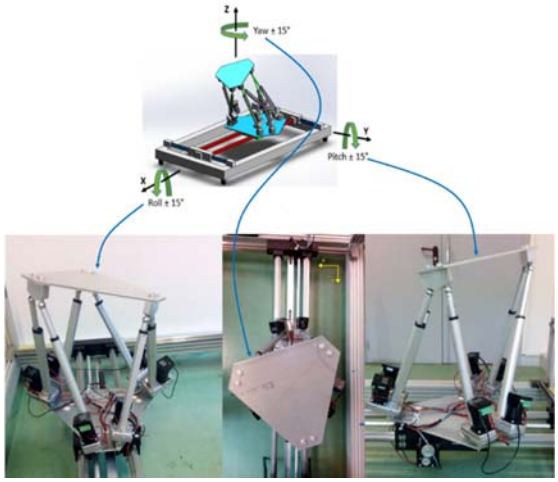


Fig. 2. The pseudo-rotation of the XY-6 DoF simulator.

2.1. Gough-Stewart Platform

The main advantage of the XY-6 DoF Simulator is that it is a completely open low-level access platform

that makes it very easy to create, develop, and evaluate new algorithms.

Our hybrid XY-6 DoF simulator takes advantage of the XY Table and the parallel Gough-Stewart platform characteristics.

Linear XY motions from the bottom of the platform and rotational motions from the upper part are generated by 8 PD4- CB Nanotec motors, guaranteeing the system a total of 6 degrees of freedom. Cylinders actuated by the six motors of the upper part allow rotational movements with an angular amplitude of +/- 15°.

The following table shows the characteristics of the XY-6 degrees of freedom in each direction.

Table 1. XY-6 DoF simulator characteristics.

Axis	Acceleration	Trajectory
X	1.25 (m/s²)	115 (cm)
Y	0.71 (m/s²)	115 (cm)
Z	0.52 (m/s²)	30 (cm)
Roll	0.17 (rad/s²)	+/- 15 (°)
Pitch	0.17 (rad/s²)	+/- 15 (°)
Yaw	0.17 (rad/s²)	+/- 15 (°)

The PD4-CB is a brushless DC motor integrating controller and absolute encoder with an incremental position encoder. The factor β of passage from the incremental position to an absolute position is 1000 for 1 centimeter.

2.2. Platform Workspace and Singularities

The workspace can generally be defined by two types of workspaces: reachable workspace and dexterous workspace. The reachable workspace is defined as the region in which every point can be reached by the upper platform in at least one orientation. In other words, only those points for which there is a solution to the inverse displacement problem are included. Fig. 3 and Fig. 4 show the translational and rotational reachable workspace of the Gough-Stewart platform used in the XY - 6 DoF.

The dexterous workspace is defined as a region of the reachable workspace in which every point can be reached by the upper platform in all possible orientations.

In this work, the reachable and dexterous workspaces of the manipulators are obtained by discretizing the region and locating all points in the region that lie within the boundaries of the corresponding workspace. The dexterous workspace is presented in Fig. 5. The purpose of adding the XY sliding axis is to increase the workspace of the Gough-stewart robot and increase its kinematic and dynamic capability. Fig. 6 shows the dexterous workspace of the XY-6 DoF platform and how the workspace is greatly increased up to ten times.

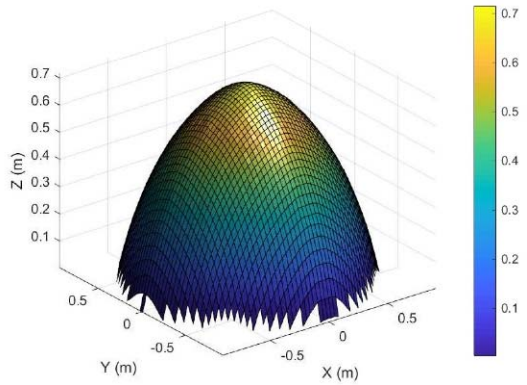


Fig. 3. Gough-Stewart reachable translation workspace.

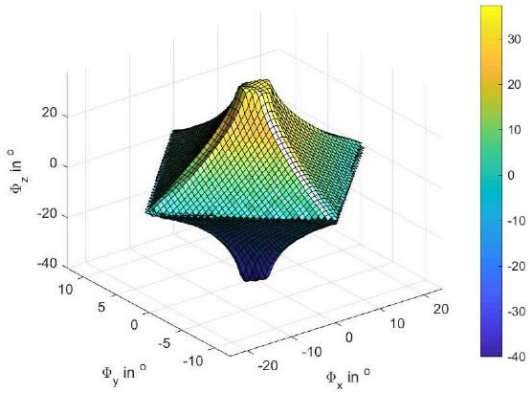


Fig. 4. Gough-Stewart rotation workspace.

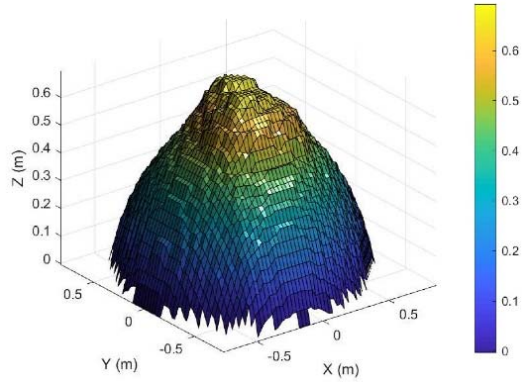


Fig. 5. Gough-Stewart dexterous workspace.

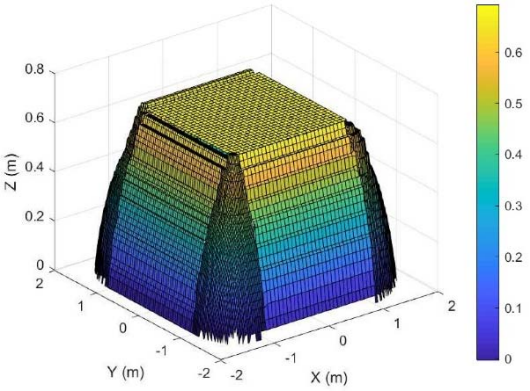


Fig. 6. Dexterous workspace of the XY-6 DoF.

Singularity equations are difficult to obtain for mechanisms with more than three degrees of freedom because the determinant of the Jacobian matrix becomes very complex. For the first time, the singularity equation for the general Gough-Stewart platform was derived from [12]. In fact, it is also a complete singularity equation because the 20 coefficients are functions of the 3 orientation angles. Later, based on the cascade expansion of the determinant of the Jacobian matrix. A procedure was developed in [13] to obtain the explicit expressions of the 20 coefficients as functions of the orientation angles. Unfortunately, the singularity equations obtained in [12, 13] are very complex because they contain too many geometrical parameters. Moreover, this method lacks flexibility because the considered point P is chosen as origin O' of the moving frame.

To solve this problem, [14] proposes that the origin O' of the moving frame should be separated from the point under consideration P and chosen to coincide with a special point on the platform in order to minimize the number of geometric parameters of the platform. Similarly, the fixed frame should also be chosen to be at a special point on the base to minimize the number of geometric parameters of the base.

Recall that, the inverse kinematics can be expressed by $J_q\dot{q} = J_x\dot{x}$ and for the parallel robot $\det(J_x) \# 0$. By using the condition for the direct singularity for our simulator (J_x = identical matrix, $J_q = {}^{R_b}J_{R_p}^{-1}$), $\det({}^{R_b}J_{R_p}^{-1} = 0)$, [14] has expressed the singularity equation as follow:

$$\begin{aligned} f_1x^3 + f_2x^2y + f_3x^2yz + f_4x^2 + f_5y^2x + f_6xyz + f_7xy \\ + f_8xz^2 + f_9xz + f_{10}x + f_{11}y^3 \\ + f_{12}y^2z + f_{13}y^2 + f_{14}yz^2 + f_{15}yz \\ + f_{16}y + f_{17}z^3 + f_{18}z^2 + f_{19}z + f_{20} \\ = 0 \end{aligned} \quad (1)$$

This is a surface of the third order in three-dimensional space, where the coefficients f_i, $i = 1, \ldots, 20$ are functions of the geometric parameters and of the orientation angles ϕ_x, ϕ_y, ϕ_z . Thus, the fi coefficients can be expressed as follows: $f_i = g(\theta_x, \theta_y, \theta_z)$ and they are explicitly presented in Jiang (2008) [93]. For the Gough-Stewart architecture (Simplified Symmetric Manipulator – Semiregular hexagons) used in the XY - 6 DoF simulator, and as recommended in [14] the reference frame O_{xyz} is attached to the base by selecting the midpoint of line segment B_1B_2 as the origin O and B_1B_2 as the x-axis. The O_{xy} plane coincides with the base plane. The mobile frame $O'_{x'y'z'}$ is attached to the platform by taking the midpoint of line segment P_1P_2 as the origin O′and P_1P_2 as the x′ axis. The $O'_{x'y'}$ plane coincides with the platform plane. Hence, the positions of B_i $(i = 1, 2, \ldots, 6)$ in the fixed frame are respectively

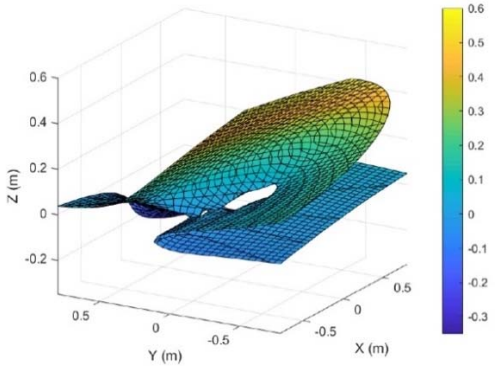
$$b_1 = [-t_1, 0, 0]^T, b_2 = [t_1, 0, 0]^T,$$
$$b_3 = [t_2, t_3, 0]^T, b_4 = [t_4, t_5, 0]^T,$$
$$b_5 = [-t_4, t_5, 0]^T, \text{and } b_6 = [-t_2, t_3, 0]^T.$$

The number of geometric parameters defining the base is only 5. Similarly, the position of P_i $(i = 1, 2, \ldots, 6)$ in the mobile frame are respectively.

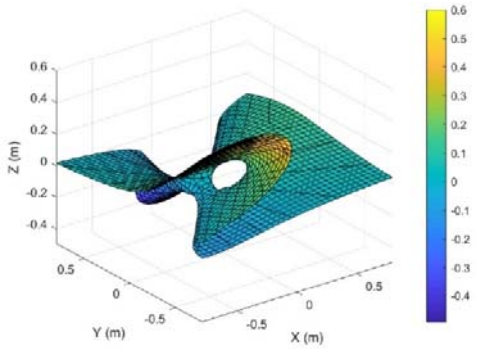
$$p'_1 = [-t_6, 0, 0]^T, p'_2 = [t_6, 0, 0]^T$$
$$p'_3 = [t_7, t_8, 0]^T, p'_4 = [t_9, t_10, 0]^T$$
$$p'_5 = [-t_9, t_10, 0]^T, \text{and } p'_6 = [-t_7, t_8, 0]^T.$$

The number of geometric parameters defining the mobile platform is also 5. Hence, the total number of geometric parameters for the hexagon used in the XY - 6 DoF is about 10.

Thanks to the equation (1), we are able to plot the Singularity loci in 3D Cartesian space with constant orientations, as shown in Fig. 7. Similarly, we have also depicted the Singularity loci in 3D Cartesian space with constant positions in Fig. 8. Additionally, we have represented the Singularity loci by defining two orientations and one position in Fig. 9.



(a) $\phi_x = \phi_z = 25^o$, $\phi_y = 25^o$



(b) $\phi_x = \phi_y = 25^o$, $\phi_z = 0^o$

Fig. 7. Singularity loci in 3D Cartesian space with constant orientations.

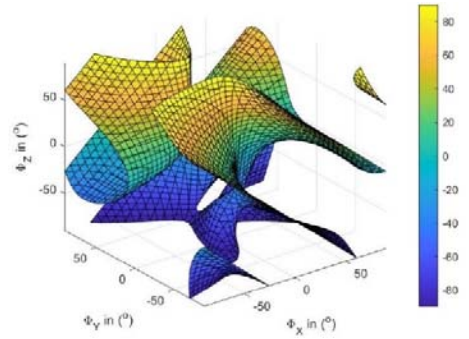


Fig. 8. (a). Singularity loci in 3D Cartesian space with constant positions. $P_0 = [0.5, 0.5, 0.5]^T$ in m.

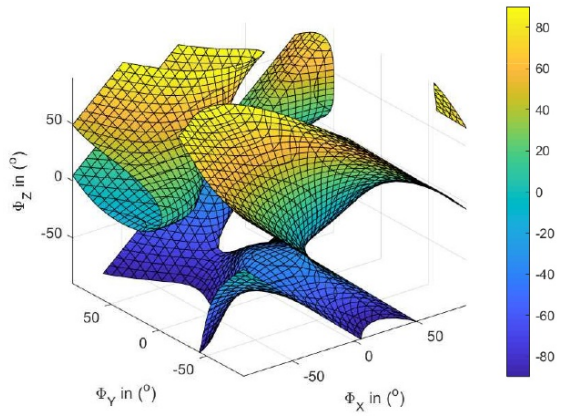
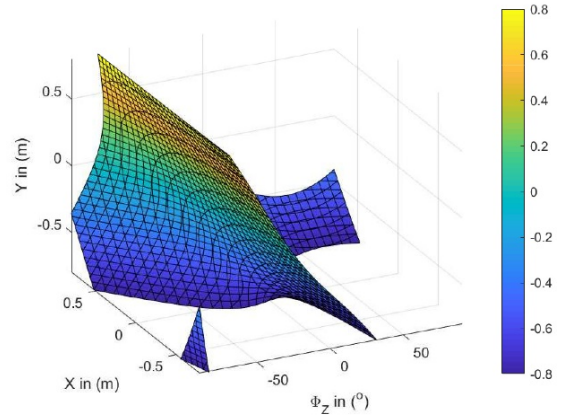
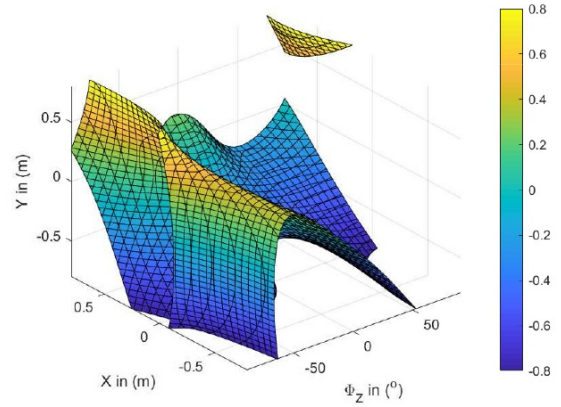


Fig. 8 (b). Singularity loci in 3D Cartesian space with constant positions. $P_0 = [0.1,\ 0.1,\ 0.1]^T$ in m.



(a) $\phi_x = \phi_y = 10^o$, z = 0.2m



(b) $\phi_x = \phi_y = 25^o$, z = 0.3m

Fig. 9. Singularity locus in 3D Cartesian space.

2.3. Platform Communication

Communication with the Gough-Stewart platform is carried out using a National Instruments card PCI - 8513 CAN, a CAN FD interface (Controller Area Network/Flexible Data-Rate). This device allows communication with the PD4-CB brushless DC motors at 1 Mbps and their control via a special Matlab toolbox. Engine communication is done in C# with the CANopen protocol, which defines motors by node IDs allowing to change and access their state and operating mode.

This protocol is based on sending 3 types of objects namely, PSO (Process Data Object), SDO (Service Data Object) and NMT (Network Management). However, an intermediate communication layer allows motor control with Matlab by mapping C# and Matlab functions. This intermediate layer makes possible to use directly from Matlab the NI PCI card to enhance the communication speed (see Fig. 10). Thus, the position instructions are sent in incremental angular position then converted into hexadecimal value in order to be adapted to the CANopen protocol.

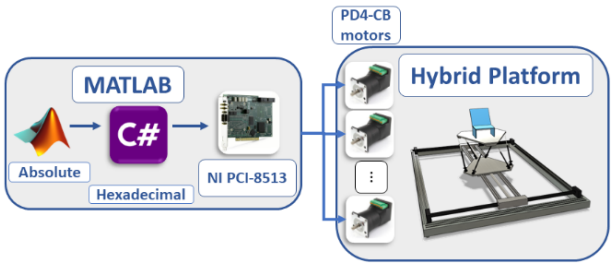


Fig. 10. Platform communication via the CANopen protocol.

The 8 joints are driven by the Nanotec PD4-CB servo motor, where the rotational movement of the leg is converted into a translational movement by the high-quality ball screw system. The motors are controllable in position, speed, and acceleration by instructions sent through the CAN bus.

2.4. Platform Security Protocol

A security protocol has been designed to guarantee the physical integrity of the platform. Each time the platform is powered up, the security protocol runs to determine the edges of the platform and define them as limited in the range of motion with a small safety gap as presented in Fig. 11.



Fig. 11. Security protocol for the platform safety area.

The protocol triggers the movement of the platform along the X-then Y axis successively with low speed. The platform's position is retrieved to determine when

the position difference Δ_p is smaller than a defined threshold value γ. The threshold value is defined as follows:

$$\gamma = 166.7\ \omega\Delta_t \quad (2),$$

where ω is the angular speed assigned to the axis motor and Δ_t the frequency of acquisition of the position. Thus, the platform's edge is assumed to be reached when the distance difference Δ_p is lower than the threshold value γ. Then, we add a safety gap of 5 centimeters at this reference 0 position to ensure a safety area. Verification protocols are built into the motion functions of the platform to ensure the desired range of motion is within the safety area.

2.5. NAO Robot

Fig. 12 presents the complete technological system architecture. illustrating the integration of the Nao robot into our immersive environment simulator XY-6 DoF. Thanks to the advantages of its pelvic kinematics design, the well-known Nao robot [15,16] was chosen to be integrated into the system, respecting the mechatronic constraints related to handi-skiing context (inactive lower limbs).

NAO is a humanoid robot with 25 DoF that includes many sensors and actuators, allowing interaction with its environment. In particular, joint sensors are Magnetic Rotary Encoders (MRE) using Hall-effect sensor technology with an accuracy of 0.1°, which provides reliable information of the angular position of the robot over time. In addition, an IMU sensor is composed of 3-axis gyrometers and accelerometers placed in the torso. A dedicated library named NAOqi provides access to sensors, system information, and actuator control.

Using ROS allows the synchronization of sensors and actuators to perform future postural control. The architecture of the entire NAO system is illustrated in Fig. 13. The connections between mechatronic and software layers presented in Fig. 5 highlight the existing multi-robot interaction and the technical methods that allow its observation.

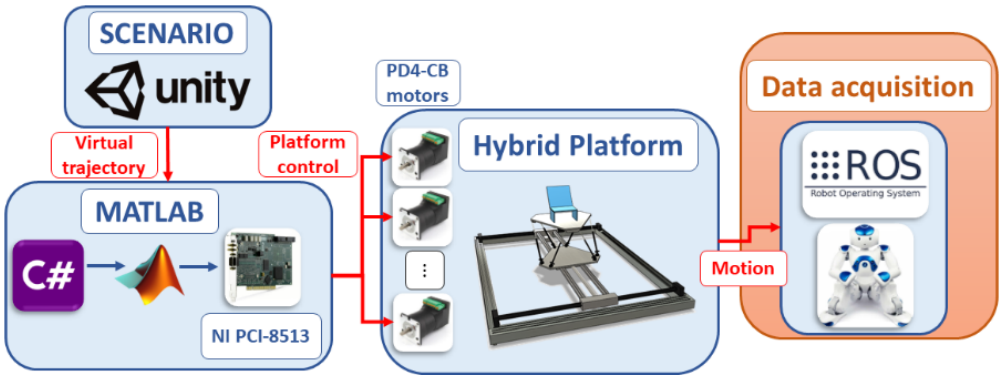


Fig. 12. Technological system architecture.

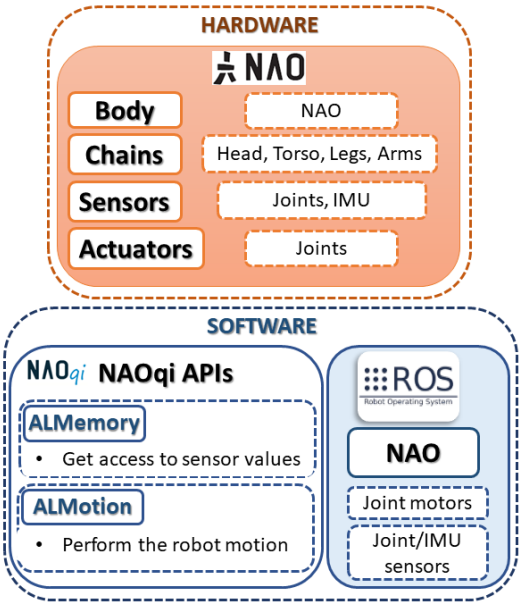


Fig. 13. Architecture of the NAO robot system.

3. Multi-robot Interaction

The XY-6 DoF platform tracks trajectory information from the virtual slide scenario designed using Unity software. The dynamic modeling behavior and sliding mode control of the XY-6 DoF robot simulator were developed and validated in a previous research work [3, 10, 17], where inertial and friction parameters were optimized and identified. The dynamics of the XY-6 DoF simulator can be represented as follows:

$$\Gamma = {}^{b}J_p^T\left({}^{b}F_e + {}^{b}F_p\right) + \sum_{i=1}^{6}\left(\frac{\partial \dot{q}_i}{\partial \dot{q}_a}\right) H_i(q,\dot{q},\ddot{q}), \quad (3)$$

where Γ is the vector of the actuator torques, ${}^{b}J_p^T$ is the Jacobian matrix, ${}^{b}F_e$ is the external wrench exerted on the platform, $\dot{q}_i$ is the passive joints speeds, $\dot{q}_a$ is the active joints speed, $H_i(q,\dot{q},\ddot{q})$ is the inverse dynamic model of leg i considering as serial robot, ${}^{b}F_p$ is the the total forces, is calculated by the following equation:

$${}^{b}F_p = {}^{b}\Pi_p\ {}^{b}\dot{v}_p + \begin{bmatrix} {}^{b}w_p \times ({}^{b}w_p \times {}^{0}MS_p) \\ {}^{b}w_p \times ({}^{b}I_p\ {}^{b}w_p) \end{bmatrix} - \begin{bmatrix} M_p I_3 \\ {}^{b}M\hat{S}_p \end{bmatrix} {}^{b}g, \quad (4)$$

where M_p, ${}^{b}\mathrm{I}_p$, ${}^{b}\Pi_p$, ${}^{0}MS_p$ are mass, inertia tensor, spatial interia matrix moment of inertia vector of the platform, respectively.

Parallel and serial robots are a known challenge which is the large number of dynamic parameters, which requires a lot of processing time, whether in dynamic modeling, identification or control. Therefore, the dynamic parameters of the XY-6 DoF hybrid structure simulator have been optimized and identified in previous works [17]. As a result, the standard 210 inertial parameters are reduced to only 90 basic inertial parameters. The motion of the XY-6 DoF simulator motion is validated by the acceleration data from the NAO IMU and the robot model, as shown in Fig. 14.

Many works [18, 19] highlight interactions in multi-modal robotic systems, such as human-robot and multi-robot interactions, to improve the collaboration and/or the impact between systems. First, the integrated system applies a validation process to the platform motion management algorithms to improve the reliability of virtual trajectory recovery. It provides a reliable solution to assess the motion control of the XY-Gought-Stewart platform and multi-robot interaction.

The interaction evaluation will be done through the inertial and articular information coming from NAO. Afterward, a human motion perception model will be integrated into the system to improve the emulation of human sensory capabilities within NAO.

Figs. 15 and 16 shows the homothety between the present integration of multi-robot interaction and the objective integration of robot-robot human interaction (outlined in red). Visual information will be exploited by a visual SLAM algorithm [20,21] that will mimic how humans perceive their movement through their eyes and the processing of information by the visual cortex. Likewise, inertial information from the NAO IMU and visual information will feed a perception model that mimics the human capacity of self-motion perception through its vestibular system and visual cortex. This future integration will provide a tool for measuring the quality of immersion for simulators by estimating through sensor data the impact of the movements of the virtual scenario and the platform on a human.

4. Experimental Results

The validation of the platform-controlled motion is illustrated in the following figures through the study of multi-robot interaction [22]. In this work, we have neglected the Z-axis and yaw rotation as they have a minor effect on the ski motion sensation comparing to the X and Y axes and roll and pitch rotation. Translation motions on axis X and Y in Fig. 17 and Fig. 18 are oscillatory movements of one meter in amplitude. Similarly, the rotational motions illustrated in Fig. 19 and Fig. 20 are oscillatory angular movements from -10 to 0 degrees. The platform behaviors are obtained by extrapolating the platform position from XY motors through the kinematic model.

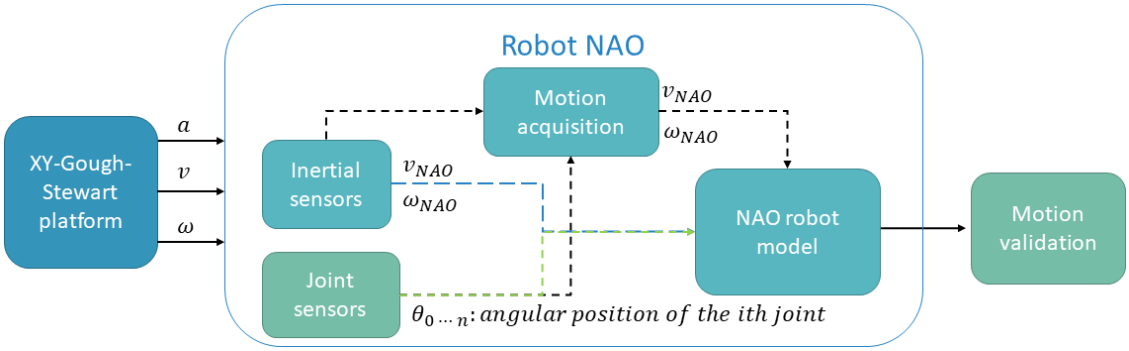


Fig. 14. XY-6 DoF simulator/NAO robot interaction.

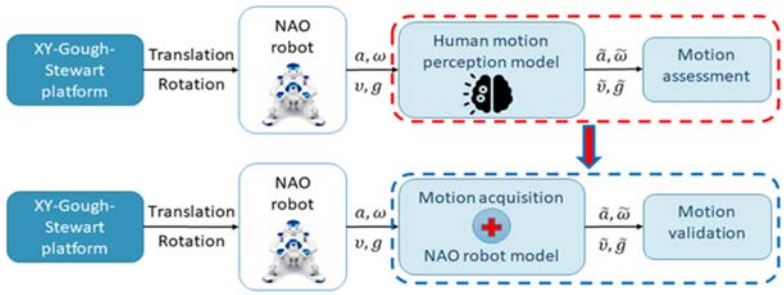


Fig. 15. Multi-robot and robotic human interaction.

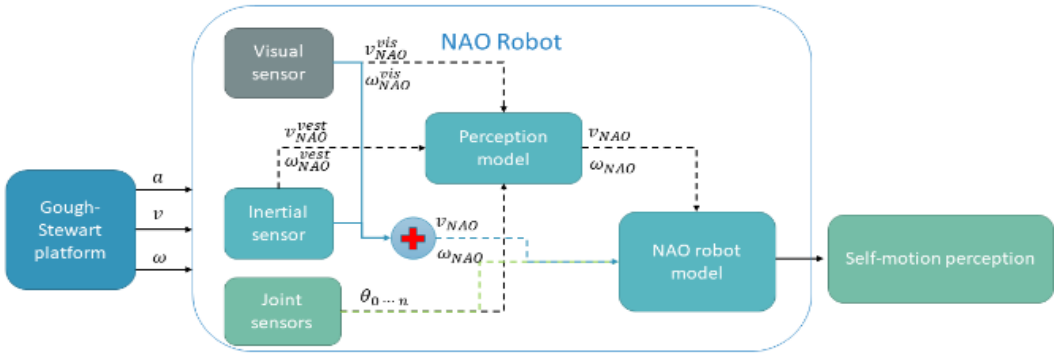


Fig. 16. Human/robot homothety for the self-motion perception.

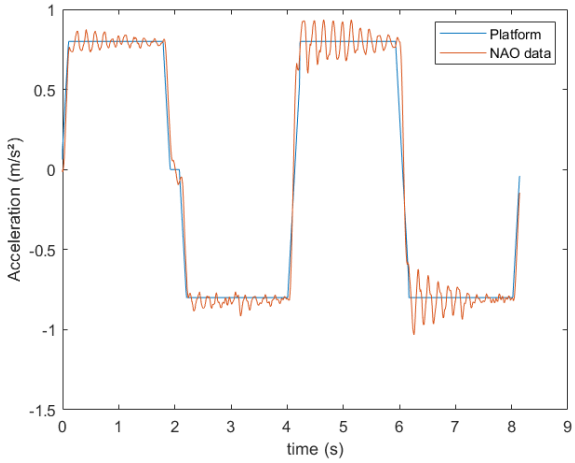


Fig. 17. Motion validation for X-axis movement.

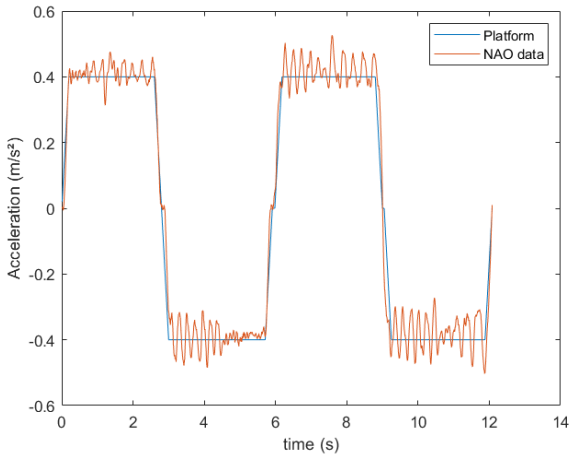


Fig. 18. Motion validation for Y-axis movement.

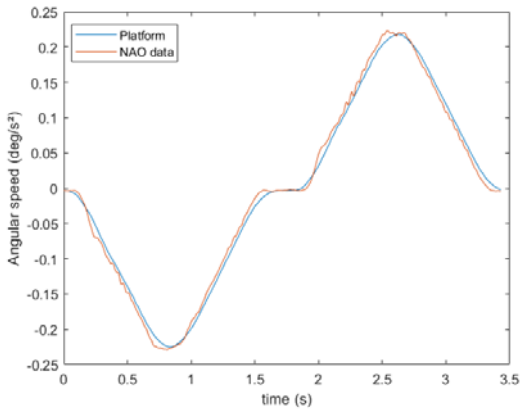


Fig. 19. Motion validation for Pitch movement.

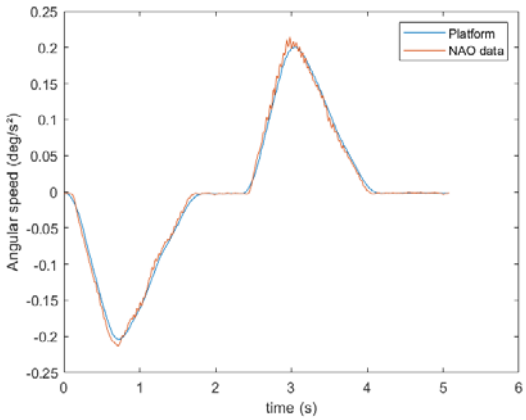


Fig. 20. Motion validation for Roll movement.

Observing the NAO robot's dynamic behavior in Fig. 17 and Fig. 18 validates the platform's accurate behavior tracking for an axis movement. However, some oscillations are observed for high dynamics. They result from slight platform vibrations due to axis friction and IMU acquisition noise.

Rotation motions do not suffer from axis friction. Thus, the angular speed behavior tracking is also precise but also less noisy.

This study validates the ability of NAO to perceive the multi-robot interaction and the interest in integrating it into our system for future work. An additional IMU sensor will be put on the NAO head to simulate the human vestibular system behavior for inertial motion perception. This device will be integrated into the ROS framework that manages the system's sensors. Likewise, a virtual scenario designed with UNITY 3D will provide the visual environment for the visual SLAM algorithm and the virtual trajectories for the platform motions restoring the sensations of acceleration.

5. Conclusion

In this paper, we introduced an original robotic platform combining the advantages of the parallel Gough-Stewart platform and an XY-table. The workspace offers by this hybrid platform is an interesting solution to enhance the motion restitution possibility. This XY-6 DoF simulator provides a comprehensive system to mimic the human self-motion perception behavior for a better immersive sliding simulator. A humanoid NAO robot is added to the upper platform to validate the platform motion acquisition through its intern inertial sensor. This robot, a real human homothetic system, provides information to assess the robot-robot interaction and system behavior properly. Experimentations confirmed the system's reliable feedback, where acceleration response shapes are concordant.

Our future work aims to manage all different parts of the system to achieve human perception integration through inertial and visual senses and realize a better immersive way. This simulator will be completed by a virtual reality scenario which will provide the trajectories to the robotic platform and restore the sensations of acceleration of the virtual trajectories.

References

[1]. Casas, Sergio, Ricardo Olanda and Nilanjan Dey, Motion Cueing Algorithms: A Review: Algorithms, Evaluation and Tuning, *International Journal of Virtual and Augmented Reality,* Vol. 1, Issue 1, 2017, pp. 90–106.

[2]. Petrović, Đorđe, Radomir Mijailović and Dalibor Pešić, How to Improve the Inclusion of Drivers with Disabilities: Measures to Enhance Accessibility, Mobility, and Road Safety, *Journal of Transportation Engineering, Part A: Systems*, 148, 10, 2022.

[3]. Houda, Taha, Lotfi Beji, Ali Amouri and Malik Mallem. Dynamic Behavior of an Interactive XY - 6 DoF Simulator for People with Reduced Mobility, in *Proceedings of the IEEE Conference on Control Technology and Applications (CCTA' 2020)*, 2020, pp. 522-527.

[4]. Nahon, Meyer A. and Lloyd D. Reid, Simulator motion-drive algorithms - A designer's perspective. *Journal of Guidance Control and Dynamics*, 13, 1990, pp. 356-362.

[5]. Pan, C. T., Pei-Yuan Sun, Hao Li, Cheng-Hsuan Hsieh, Zheng-Yu Hoe and Yow-Ling Shiue. Development of Multi-Axis Crank Linkage Motion System for Synchronized Flight Simulation with VR Immersion. *Applied Sciences,* 11, 2021, p. 3596.

[6]. Wei, Ming-Yen, Design and Implementation of Inverse Kinematics and Motion Monitoring System for 6DoF Platform, *Applied Sciences*, 11, 19, 2021, 9330.

[7]. Reymond, Gilles and Andras Kemeny, Motion Cueing in the Renault Driving Simulator, *Vehicle System Dynamics,* 34, 2000, pp. 249 - 259.

[8]. Salaani, Mohamed Kamel, Dennis Guenther and Gary Heydinger, Vehicle dynamics modeling for the national advanced driving simulator of a 1997 jeep Cherokee, *SAE Transactions*, 108, 1999, pp. 443-465.

[9]. Miunske, Tobias, Christian Holzapfel, Edwin Baumgartner and Hans-Christian Reuss. A new Approach for an Adaptive Linear Quadratic Regulated Motion Cueing Algorithm for an 8 DoF Full Motion Driving Simulator, in *Proceedings of the International Conference on Robotics and Automation (ICRA' 2019),* 2019, pp. 497-503.

[10]. Houda, Taha, Lotfi Beji, Ali Amouri and Malik Mallem. Handiski simulator performance under PSO-based washout and control parameters optimization. *Nonlinear Dynamics,* 110, 2022, pp. 649 - 667.

[11]. Amouri, Ali and Fakhreddine Ababsa. Sliding Movement Platform for Mixed Reality Application, *IFAC-PapersOnLine*, 49, 2016, pp. 662-667.

[12]. St-Onge B. M., Gosselin C. M., Singularity Analysis and Representation of the General Gough-Stewart Platform, *The International Journal of Robotics Research*, 19, 3, 2000, pp. 271-288.

[13]. Li, H., Gosselin, C. M., Richard, M. J., and St-Onge, B. M., Analytic Form of the Six-Dimensional Singularity Locus of the General Gough - Stewart Platform, *ASME. J. Mech. Des.,* 128, 1, January 2006, pp. 279–287.

[14]. Q. Jiang, Singularity-free Workspace Analysis and Geometric Optimization of Parallel Mechanisms, PhD thesis, *Laval University*, Quebec, QC, Canada, October 2008.

[15]. Gouaillier, David, Vincent Hugel, Pierre Blazevic, Chris Kilner, Jérôme Monceaux, Pascal Lafourcade, Brice Marnier, Julien Serre and Bruno Maisonnier. Mechatronic design of NAO humanoid, in *Proceedings of the 2009 IEEE International Conference on Robotics and Automation*, 2009, pp. 769-774.

[16]. Kofinas, Nikolaos, Emmanouil Orfanoudakis and Michail G. Lagoudakis. Complete Analytical Forward and Inverse Kinematics for the NAO Humanoid Robot, *Journal of Intelligent & Robotic Systems,* 77, 2015, pp. 251-264.

[17]. Houda, Taha, Ali Amouri, Lotfi Beji and Malik Mallem. Dynamic Parameters Optimization and Identification of a Parallel Robot, *Multibody Dynamics*, 2019, 53, 2019, pp. 367-374.

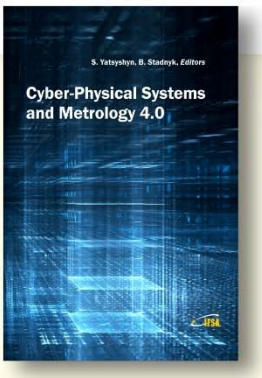
[18]. Darmanin, Rachael N. and Marvin K. Bugeja. A review on multi-robot systems categorised by application domain, in *Proceedings of the 25th Mediterranean Conference on Control and Automation (MED' 2017),* 2017, pp. 701-706.

[19]. Sharkawy, Abdel-Nasser, Human-Robot Interaction: Applications, in *Proceedings of the 1st IFSA Winter Conference on Automation, Robotics & Communications for Industry 4.0,* February 2021, pp. 98-103.

[20]. Bescos, B., Fácil, J. M., Civera, J., and Neira, J., DynaSLAM: Tracking, mapping, and inpainting in dynamic scenes, *IEEE Robotics and Automation Letters*, 3, 4, 2018, pp. 4076-4083.

[21]. Beghdadi, Ayman, Malik Mallem, and Lotfi Beji, D2SLAM: Semantic visual SLAM based on the influence of Depth for Dynamic environments, *arXiv:2210.08647*, 2022.

[22]. Houda Taha, Beghdadi Ayman, Beji Lotfi and Amouri Ali, Complex Multi Robot Hybrid Platform for Augmented Virtual Skiing Immersion, in *Proceedings of the 3rd IFSA Winter Conference on Automation, Robotics & Communications for Industry 4.0/5.0 (ARCI'2023).* 2023, pp. 95-99.



Cyber-Physical Systems and Metrology 4.0

S. Yatsyshyn and B. Stadnyk, Editors

The book is written by 30 authors whose scientific achievements for the last 5 years cover a significant information technology and measurement science areas.

The purpose of this title is to present and consider the main trends in the field of metrology of Cyber-Physical Systems, which are becoming a key element of everyday life. At the first, the book is intended for engineers, lecturers, students, persons who are not acquainted enough with the specificity of Cyber-Physical Systems and their Metrology, but are interested in it.

Formats: hardcover (print book) and PDF, 332 pages
ISBN: 978-84-09-26899-3, e-ISBN: 978-84-09-26898-6

IFSA Publishing

https://www.sensorsportal.com/HTML/BOOKSTORE/Cyber-Physical_Systems_and_Metrology_4_0.htm

